Human TRPC6 expressed in HEK 293 cells forms non-selective cation channels with limited Ca^{2+} permeability

Mark Estacion[1], William G. Sinkins[2], Stephen W. Jones[2], Milana A. B. Applegate[1] and William P. Schilling[1,2]

[1] *Rammelkamp Center for Education and Research, MetroHealth Medical Center, Cleveland, OH 44109, USA*
[2] *Department of Physiology and Biophysics, Case Western Reserve University School of Medicine, Cleveland, OH 44106, USA*

TRPC6 is thought to be a Ca^{2+}-permeable cation channel activated following stimulation of G-protein-coupled membrane receptors linked to phospholipase C (PLC). TRPC6 current is also activated by exogenous application of 1-oleoyl-acetyl-*sn*-glycerol (OAG) or by inhibiting 1,2-diacylglycerol (DAG) lipase activity using RHC80267. In the present study, both OAG and RHC80267 increased whole-cell TRPC6 current in cells from a human embryonic kidney cell line (HEK 293) stably expressing TRPC6, but neither compound increased cytosolic free Ca^{2+} concentration ($[Ca^{2+}]_i$) when the cells were bathed in high-K^+ buffer to hold the membrane potential near 0 mV. These results suggested that TRPC6 channels have limited Ca^{2+} permeability relative to monovalent cation permeability and/or that Ca^{2+} influx via TRPC6 is greatly attenuated by depolarization. To evaluate Ca^{2+} permeability, TRPC6 currents were examined in extracellular buffer in which Ca^{2+} was varied from 0.02 to 20 mM. The results were consistent with a pore-permeation model in which Ca^{2+} acts primarily as a blocking ion and contributes only a small percentage (∼4%) to whole-cell currents in the presence of extracellular Na^+. Measurement of single-cell fura-2 fluorescence during perforated-patch recording of TRPC6 currents showed that OAG increased $[Ca^{2+}]_i$ 50–100 nM when the membrane potential was clamped at between −50 and −80 mV, but had little or no effect if the membrane potential was left uncontrolled. These results suggest that in cells exhibiting a high input resistance, the primary effect of activating TRPC6 will be membrane depolarization. However, in cells able to maintain a hyperpolarized potential (e.g. cells with a large inwardly rectifying or Ca^{2+}-activated K^+ current), activation of TRPC6 will lead to a sustained increase in $[Ca^{2+}]_i$. Thus, the contribution of TRPC6 current to both the kinetics and magnitude of the Ca^{2+} response will be cell specific and dependent upon the complement of other channel types.

(Resubmitted 6 December 2005; accepted after revision 25 January 2006; first published online 26 January 2006)
Corresponding author W. P. Schilling: Rammelkamp Center for Education and Research, Room R-322, MetroHealth Medical Center, 2500 MetroHealth Drive, Cleveland, OH 44109-1998, USA. Email: wschilling@metrohealth.org

The transient receptor potential (TRP) family of cation channels plays a fundamental role in signal transduction in response to a variety of stimuli including hormones and paracrine factors, temperature, pH, osmolarity and oxidative stress (for recent reviews see Clapham, 2003; Montell, 2005). TRPC6, a member of the canonical TRPC subfamily, is activated following stimulation of G-protein-coupled membrane receptors linked to phospholipase C (PLC). Along with TRPC3 and TRPC7, TRPC6 can be activated by exogenous application of 1,2-diacylglycerol (DAG), but not by intracellular dialysis of the cell with inositol 1,4,5-trisphosphate or by depletion of internal Ca^{2+} stores (Okada *et al.* 1999; Hofmann *et al.* 1999; Inoue *et al.* 2001; Estacion *et al.* 2004). Thus, TRPC6 is not considered to be a store-operated channel. Messenger RNA for TRPC6 is found in a variety of tissues including brain, kidney, lung, heart, ovary and testis (Garcia & Schilling, 1997; Riccio *et al.* 2002). Knock-down strategies have implicated TRPC6 channel in receptor-dependent responses in rabbit portal vein smooth muscle cells (Inoue *et al.* 2001), rat cerebral arteries (Welsh *et al.* 2002), smooth muscle from the rat pulmonary artery (Yu *et al.* 2003) and Jurkat T lymphocytes (Tseng *et al.* 2004), and responses that may be related to activity of TRPC6 channels have been described in PC-12 cells (Tesfai *et al.* 2001), airway smooth muscle cells (Corteling *et al.* 2004), MDCK cells (Bandyopadhyay *et al.* 2005), platelets (Hassock *et al.* 2002) and A7r5 cells, which are derived from smooth muscle (Jung *et al.* 2002). In mouse primary erythroid cells, TRPC6 interacts with TRPC2, the channel responsible for Ca^{2+} influx in response to stimulation by erythropoietin (Chu *et al.* 2004). Thus, TRPC6 channel

 DOI: 10.1113/jphysiol.2005.103143

has widespread distribution and undoubtedly plays an important role in the cellular and tissue response to various stimuli. However, the actual composition of native TRPC channels remains unknown. There is evidence that TRPC channels form heteromultimers with other members of the TRPC family (Strubing *et al.* 2001; Hofmann *et al.* 2002; Goel *et al.* 2002; Bandyopadhyay *et al.* 2005) and perhaps with other members of the larger TRP superfamily, and accessory proteins may play an important role in channel expression, targeting and regulation.

Over-expression of TRPC6 channels in HEK 293 (Inoue *et al.* 2001; Dietrich *et al.* 2003), COS-7 (Boulay *et al.* 1997; Zhang & Saffen, 2001) and CHO-K1 cells (Hofmann *et al.* 1999) is associated with an enhanced Ca^{2+} influx as indicated by fluorescent Ca^{2+} dyes, suggesting that these channels may be Ca^{2+} permeable. However, the data from electrophysiological studies are unclear on this point. Heterologous TRPC6 currents have been characterized in different cell types and are clearly activated by receptor stimulation and exogenous application of DAG analogues (Hofmann *et al.* 1999; Inoue *et al.* 2001; Estacion *et al.* 2004). Inward TRPC6 current is greatly attenuated by replacement of monovalent cations in the bath by the large relatively impermeant cation, *N*-methyl-D-glucamine (NMDG) and the reversal potential shifts to negative values demonstrating that TRPC6 channel has permselectivity expected for a non-selective cation channel. However, replacement of monovalent cations in the bath solution by Ca^{2+} causes substantial reduction in outward current via TRPC6 channels (Inoue *et al.* 2001), suggesting that Ca^{2+} may act as a channel blocker. In a recent study, increases in Ca^{2+} from the normal value of 2 mM to 10 mM in the presence of Na^+ produced a substantial reduction in TRPC6 inward current (Shi *et al.* 2004), again suggesting channel block. However, the actual percentage of whole-cell TRPC6 currents attributable to Ca^{2+} influx in the presence of normal extracellular Na^+ remains unknown. Therefore, the purpose of the present study was to compare receptor-mediated changes in Ca^{2+} influx measured using fura-2 with changes in membrane currents in cells expressing human TRPC6 channels. Fura-2 measurements were performed on dispersed cells in a cuvette-based assay, and TRPC6 currents were measured using the patch-clamp technique in whole-cell recording mode. In addition, simultaneous recordings of TRPC6 current and fura-2 fluorescence were obtained at the single-cell level using the perforated-patch technique and fluorescence video microscopy. The results are consistent with a pore permeation model in which Ca^{2+} acts primarily as a blocking ion and contributes only a small percentage to whole-cell currents in the presence of Na^+. Furthermore, Ca^{2+} entry via TRPC6 was greatly attenuated by depolarization. Thus, in cells with a high input resistance, activation of TRPC6 current will primarily cause depolarization, greatly attenuating Ca^{2+} entry via TRPC6 channels. However, in cells able to maintain a negative membrane potential, for example, cells with a robust Ca^{2+}-activated or inwardly rectifying K^+ current, the depolarizing effect of TRPC6 will be reduced and the driving force for Ca^{2+} entry will be enhanced. In this way, TRPC6 current will serve a dual signalling role (i.e. depolarization *versus* sustained Ca^{2+} entry) that will be cell specific and dependent upon the complement of other channel types. A preliminary report of this work has been published (Estacion *et al.* 2005).

Methods

Solutions and reagents

Normal Hepes-buffered saline (HBS) contained (mM): NaCl 140, KCl 5, $MgCl_2$ 1, $CaCl_2$ 1.8, D-glucose 10 and Hepes 15 with 0.1% bovine serum albumin; pH was adjusted to 7.4 at 37°C with NaOH. Ca^{2+}-free–high-K^+ HBS contained (mM): KCl 145, $MgCl_2$ 1 EGTA 0.3, D-glucose 10 and Hepes 15 with 0.1% bovine serum albumin; pH was adjusted to 7.4 at 37°C with NaOH. RHC80267, U73122 and U73343 were obtained from Calbiochem. Fura-2 acetoxymethyl ester (fura-2 AM) was obtained from Molecular Probes. 1-oleoyl-acetyl-*sn*-glycerol (OAG), obtained from Sigma in single-use aliquots, was dissolved in ethanol at a final concentration of 30 mM and used immediately for experimentation. All other salts were of reagent grade.

Cell culture

HEK 293 cells were grown at 37°C in monolayer culture in a humidified air atmosphere with 5% CO_2 using minimal essential medium or Dulbecco's modified Eagle's medium supplemented with 2 mM L-glutamine, 10% heat-inactivated fetal bovine serum and 1% penicillin-streptomycin-neomycin antibiotic mixture (GIBCO).

Expression of TRPC6 in mammalian cells

The transfection and clonal selection of cell lines stably expressing human TRPC6 channels was previously described (Estacion *et al.* 2004). Unless otherwise indicated, all experiments reported here were performed using TRPC6-clone 14 cells, serially cultured under continuous selection pressure with G418.

Measurement of free cytosolic Ca^{2+} concentration

Cuvette experiments. $[Ca^{2+}]_i$ was measured using the fluorescent indicator, fura-2, as previously described (Schilling *et al.* 1989). Briefly, cells were harvested and re-suspended in HBS containing 20 μM fura-2 AM.

Following 30-min incubation at 37°C, the cell suspension was diluted ∼10-fold with HBS, incubated for an additional 30 min, washed and resuspended in fresh HBS. Aliquots from this final suspension were washed twice immediately prior to fluorescence measurement and resuspended in Ca^{2+}-free–high-K^+ HBS. Fluorescence was recorded in a mechanically stirred cuvette using an SLM 8100 spectrophotofluorometer. For measurements of $[Ca^{2+}]$, excitation wavelength alternated between 340 and 380 nm every second, and fluorescence intensity was monitored at an emission wavelength of 510 nm. Calibration of the fura-2 associated with the cells was accomplished with lysis by Triton X-100 in the presence of a saturating concentration of Ca^{2+} followed by addition of EGTA (pH 8.5). $[Ca^{2+}]_i$ was calculated using the equations of Grynkiewicz *et al.* (1985) using a K_d value for Ca^{2+} binding to fura-2 of 224 nM. All measurements were performed at 37°C.

Imaging experiments. Fura-2-loaded HEK 293 cells attached to glass coverslips were mounted in a perfusion chamber and placed on the stage of a Leica DMIRE2 inverted microscope. The cells were illuminated with light from a 175-W xenon lamp using a filter cube and dichroic mirror appropriate for fura-2. Excitation wavelength alternated between 340 and 380 nm using a Sutter filter wheel and appropriate filters. Epifluorescence was recorded using a SPOT-RT camera (Diagnostic Instruments, Sterling Heights, MI, USA) and images were acquired and analysed using SimplePCI imaging software (Compix Inc., Cranberry Township, PA, USA). Fura-2 calibration was performed using acquisition parameters identical to those used in each experiment, by recording the fluorescence from a solution containing fura-2 and either saturating or zero Ca^{2+} concentrations. All fura-2 imaging experiments were performed at room temperature (∼22°C). For statistical purposes, $[Ca^{2+}]_i$ responses from individual cells on each coverslip were averaged. In general, the number of cells imaged per coverslip was 10–20. The average values from multiple coverslips were averaged and reported as mean ± S.E.M. with n equal to the number of coverslips.

Electrophysiological techniques

The giga-seal technique for current recording was utilized in the whole-cell mode. All experiments were performed on HEK 293 cells attached to circular glass coverslips which were transferred to a perfusable recording chamber on the stage of a Nikon inverted microscope immediately before use. Na^+-containing Ringer solution was used as the extracellular solution and contained (mM): NaCl 160, KCl 4, $CaCl_2$ 2, $MgCl_2$ 1 and Hepes 10; pH 7.4. The pipette solution contained (mM): caesium aspartate 145, $MgCl_2$ 2, $CaCl_2$ 0.3, EGTA 10 and Hepes 10; pH 7.2 and pCa 8. In some experiments, Na^+, or Na^+ and K^+ in the Ringer solution was isosmotically replaced by NMDG. Where indicated, $[Ca^{2+}]$ in the extracellular solution was varied from 0.02 to 20 mM by replacement of either Na^+ or NMDG. Data were obtained using an Axopatch 200A amplifier (Pacer Scientific, Los Angeles, CA, USA) and sampled on-line using pCLAMP 8.0 software. The ground electrode was an Ag–AgCl wire connected to the bath via an agar bridge containing 150 mM NaCl. All recordings were made at room temperature. Electrode resistances ranged from 2 to 6 MΩ and whole-cell series resistances ranged from 4 to 20 MΩ. To generate current–voltage (I–V) relationships, voltage ramps from −120 to +120 mV over 200 ms were repetitively applied at 15-s intervals. Unless otherwise indicated, the holding potential between ramps was −50 mV and the currents were not leak-subtracted. All Figures show representative traces corrected for liquid junction potential. Where indicated, whole-cell membrane currents were also recorded using the perforated-patch technique as previously described (Korn & Horn, 1989). Pipettes were back-filled with pipette solution containing amphotericin-B. Following seal formation in cell-attached mode, the input resistance was continuously monitored. Experimental protocols were initiated when the access resistance reached a value of 40 MΩ.

Current simulations and modelling

The effect of changes in extracellular Ca^{2+} on TRPC6 currents was simulated based on a single-site, two-barrier pore model (Hille, 2001). Specifically, an Excel spreadsheet was used to calculate I–V relationships from the analytical solution to the model (eqn (15.10) of Hille, 2001; with equilibrium constants and maximal currents defined using eqns (15.8) and (15.9) and rate constants at 0 mV calculated as in eqn (15.11) with a pre-exponential factor of 6.11×10^{12}). Parameters of the model (free energy levels for the barriers and binding site for Ca^{2+} and for monovalent cations, and the fractional electrical distance from the outside to the binding site (δ)) were adjusted manually to fit the experimental data (i.e. to best approximate the shape of the I–V plot and shifts in reversal potential). Parameter values are given in the legend to Fig. 5 (see also inset to Fig. 5*B*). The barriers were placed at the inner and outer edges of the membrane, so ion entry rates were voltage-independent. The rate constants for ion exit to the extracellular (k_e) and intracellular (k_i) sides were:

$$k_e = k_{0e}\, e^{\delta_z FV/RT} \quad \text{and} \quad k_i = k_{0i}\, e^{(\delta-1)_z FV/RT}$$

where k_{0e} and k_{0i} are the rate constants at 0 mV, z is the valence of the ion, F and R are gas law constants, V is the

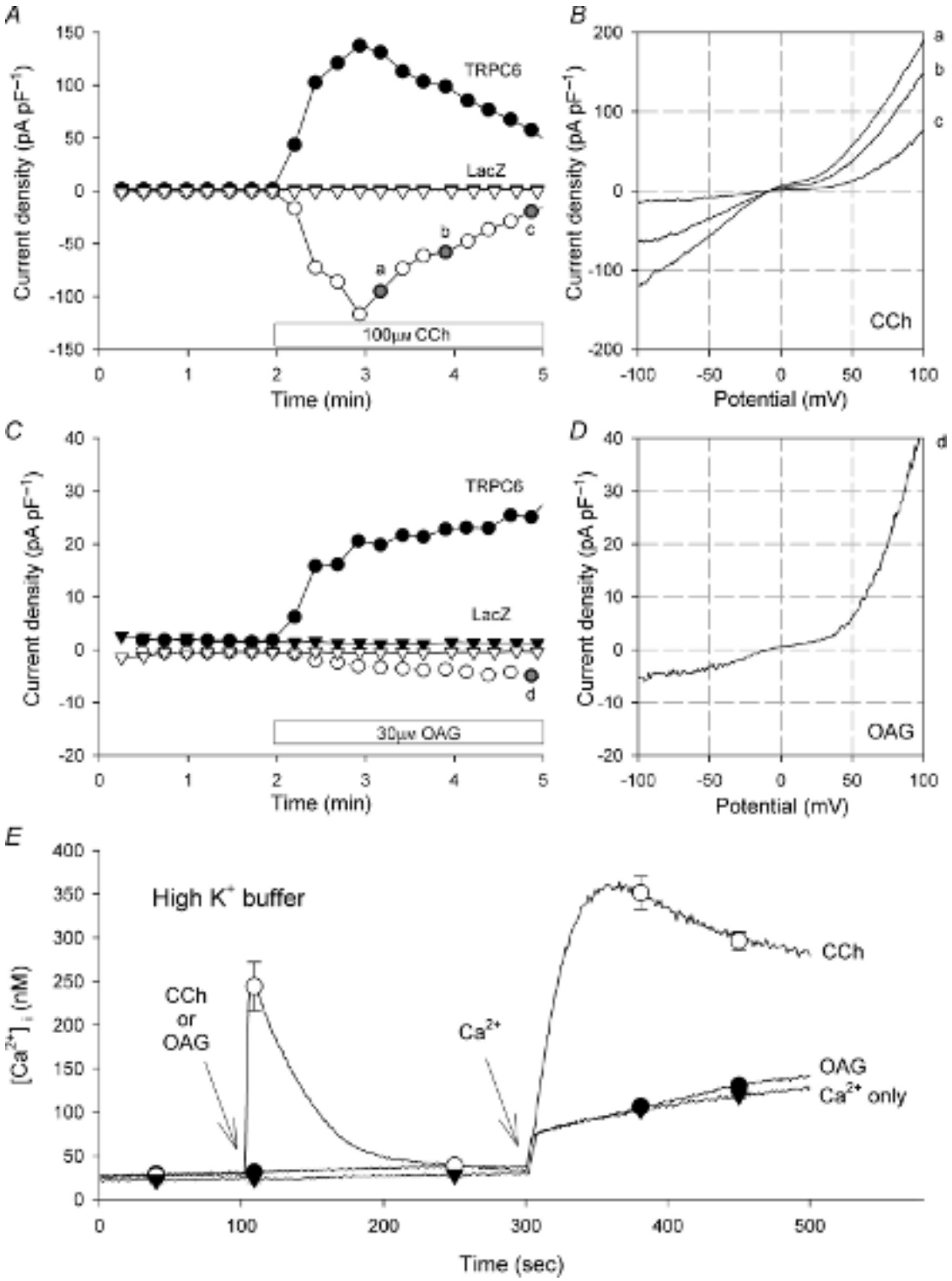

Figure 1. Stimulation of TRPC6 channels expressed in HEK 293 cells
*A, w*hole-cell membrane currents were recorded in TRPC6-expressing HEK 293 cells (circles) or lacZ-transfected control cells (inverted triangles) as described in the Methods. Voltage ramps were applied every 15 s and the outward current at +80 mV (filled symbols) and inward current at −80 mV (open symbols) during each ramp is plotted as a function of time after rupture of the patch for whole-cell recording. At the time indicated by the horizontal bar, the bath solution was changed to one containing carbachol (CCh; 100 μM). *B*, current–voltage (*I–V*) relationships obtained in the presence of CCh at the times indicated (a, b and c) in *A*. *C* and *D*, same as in *A* and *B* with OAG added at the time indicated by the horizontal bar. *I–V* relationship was obtained at the time

membrane potential and T is the absolute temperature. To account for the small inward current seen in 0.02 mM extracellular Ca^{2+}, the contribution of leak current and the permeability of TRPC6 channels for NMDG in the simulations was set at 5% of the Na^+ permeability; Na^+, K^+ and Cs^+ were treated as identical. The same model parameters were used to simulate the entire data set. The relative permeability of TRPC6 channels for Ca^{2+} *versus* monovalent cation was determined using the equations of Frazier *et al.* (2000).

Results

Activation of human TRPC6 by receptor stimulation and OAG

TRPC6 channel activity was recorded using the patch-clamp technique in whole-cell recording mode. The pipette solution contained a high concentration of EGTA (10 mM) to buffer Ca^{2+} (pCa ~8) and no ATP or GTP. The major cation in the pipette solution was Cs^+ and the monovalent cations in the extracellular bath were Na^+ and K^+. Additionally, the bath solution contained 2 mM Ca^{2+}. Under these conditions, exposure of HEK 293 cells stably expressing human TRPC6 to carbachol (CCh) ~2 min after initiating whole-cell dialysis via the patch pipette, caused a time-dependent activation of membrane current (Fig. 1*A*) with distinctive inward and outward rectification properties as seen in the *I–V* relationship (Fig. 1*B*). Current increased to a peak value within ~1 min and subsequently declined slowly with time. As previously reported (Hofmann *et al.* 1999; Inoue *et al.* 2001; Estacion *et al.* 2004), application of OAG also increased TRPC6 current (Fig. 1*C* and *D*), but the response developed more slowly and the current density were less than that observed with CCh. Neither CCh- nor OAG-induced currents were observed in lacZ-transfected control HEK 293 cells. It is important to note that under these ionic conditions, outward current is primarily carried by Cs^+, inward current is carried by Na^+, K^+ and Ca^{2+}, and the current reversal potential is slightly negative (−10 mV). Although the proportion of inward current carried by each ion has not been determined, previous experiments have estimated the permeability ratio of $Na^+ : Cs^+ : K^+ : Ca^{2+}$ for the TRPC6 channel to be approximately 1 : 0.8 : 1 : 5 (Hofmann *et al.* 1999; Inoue *et al.* 2001).

We next examined the ability of CCh and OAG to increase Ca^{2+} influx in the TRPC6-expressing HEK 293 cells (Fig. 1*E*). Cells were loaded with fura-2 and suspended in a cuvette in 0-Ca^{2+} buffer in which the normal Na^+ was replaced by K^+ (i.e. Ca^{2+}-free–high-K^+ HBS) to essentially clamp the membrane potential at zero. Under these conditions, addition of a maximum concentration of CCh caused a transient increase in $[Ca^{2+}]_i$ indicative of the release of Ca^{2+} from internal stores. Re-admission of Ca^{2+} (10 mM) to the extracellular solution following addition of CCh caused a large and rapid increase in $[Ca^{2+}]_i$ indicative of Ca^{2+} influx. This increase in $[Ca^{2+}]_i$ presumably reflects the activation of both endogenous receptor- or store-operated Ca^{2+} entry pathways present in HEK 293 cells, and heterologously expressed TRPC6 channels. In sharp contrast, addition of 100 μM OAG, a maximum concentration for activation of TRPC6 current (Estacion *et al.* 2004), had no acute effect on $[Ca^{2+}]_i$ and subsequent re-admission of Ca^{2+} to the bath produced a response that was not significantly different from basal Ca^{2+} influx determined by Ca^{2+} re-admission in the absence of either CCh or OAG. Thus, despite the fact that both OAG and CCh activate TRPC6 whole-cell currents, OAG had no discernable effect on $[Ca^{2+}]_i$, suggesting that the CCh-induced change in $[Ca^{2+}]_i$ observed in these experiments is unrelated to TRPC6 channel activation.

Effect of RHC80267

Previous studies have shown that the DAG lipase inhibitor, RHC80267 (RHC), which is thought to increase both basal and receptor-stimulated DAG levels, increases $[Ca^{2+}]_i$ and whole-cell currents in cells over-expressing TRPC6 channel (Hofmann *et al.* 1999; Inoue *et al.* 2001). We therefore examined the effect of RHC on membrane currents and $[Ca^{2+}]_i$ in TRPC6-expressing cells. Addition of RHC to the bath solution produced a time- and concentration-dependent increase in TRPC6 current. The current activation rate and magnitude were similar to that observed with OAG (Fig. 2*A* and *B*). In contrast, addition of RHC to the extracellular solution (Ca^{2+}-free–high-K^+ HBS) had no effect on basal $[Ca^{2+}]_i$ and re-admission of Ca^{2+} produced a response that was not significantly different from basal influx (Fig. 2*C* and *D*). Thus it would appear that inhibition of DAG lipase does not stimulate Ca^{2+} influx in TRPC6-expressing cells. We next determined whether RHC could enhance CCh-induced responses. As seen in Fig. 2*C* and *D*, RHC decreased CCh-induced release of Ca^{2+} from internal

indicated (d) in *C*. *E*, fura-2-loaded HEK 293 cells stably expressing TRPC6 were suspended in Ca^{2+}-free–high-K^+ HBS and the fluorescence ratio was recorded as a function of time as described in the Methods. Three traces are shown superimposed. CCh (100 μM; ○) or OAG (100 μM; ●) was added to the cuvette at the time indicated by the arrow. Ca^{2+} (10 mM) was added in all cases at 300 s. The third trace shows the addition of Ca^{2+} alone at 300 s (▼). Curves represent mean values of three independent experiments; symbols represent mean ± S.E.M. values at selected time points.

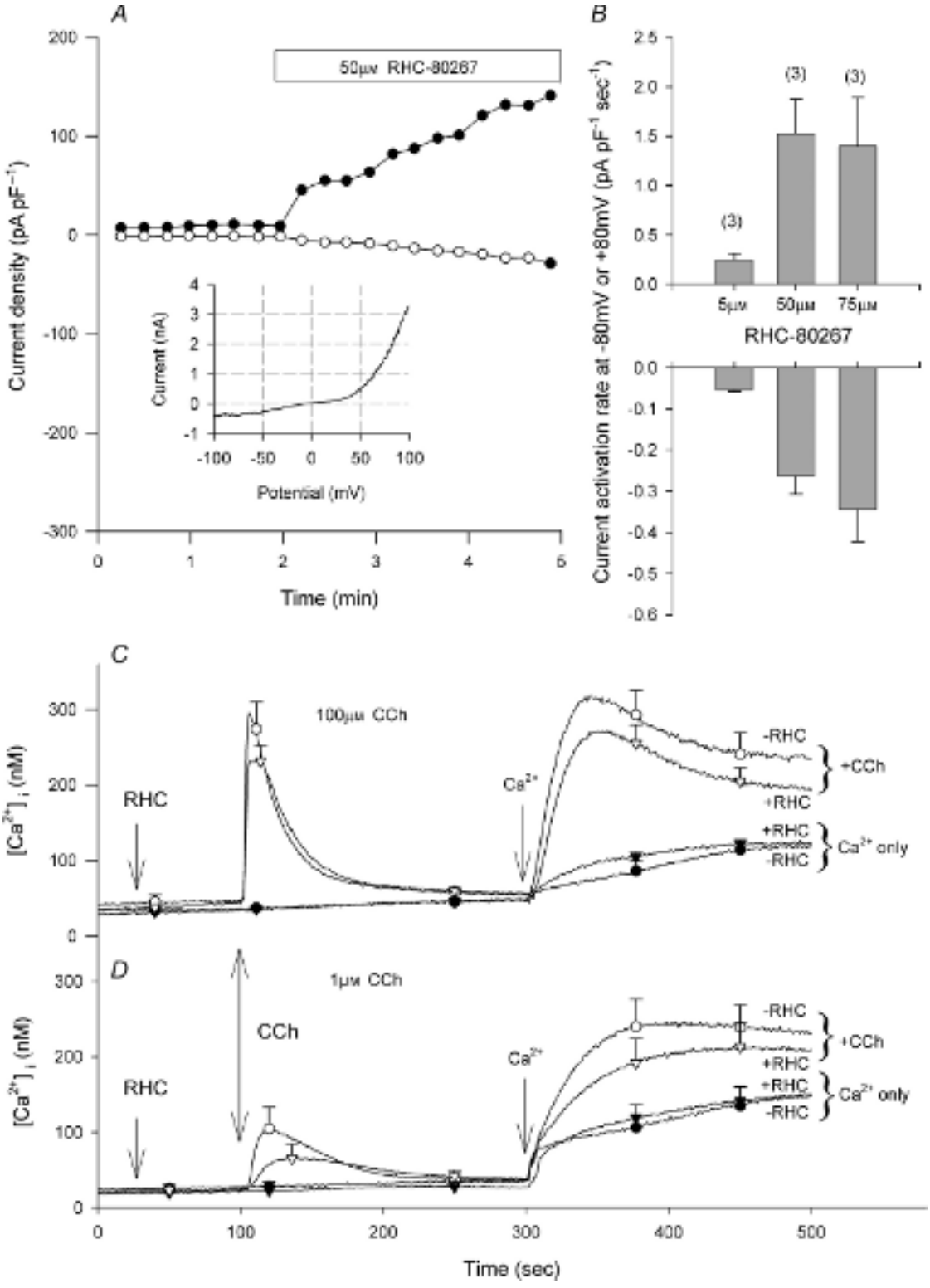

Figure 2. Stimulation of TRPC6 by the DAG lipase inhibitor, RHC80267
A, whole-cell membrane currents were recorded in TRPC6-expressing HEK 293 cells as described in the legend to Fig. 1. At the time indicated by the horizontal bar, the bath solution was changed to one containing RHC80267 (RHC; 50 μM). Inset shows the *I–V* relationship at 5 min. *B*, mean ± S.E.M outward (upward bars) and inward (downward bars) current activation rates following the addition of RHC as shown in *A* at the indicated concentrations. The numbers in parentheses indicate the number of individual cells tested. *C*, fura-2-loaded HEK 293 cells stably expressing TRPC6 channels were suspended in Ca^{2+}-free–high-K^+ HBS. Four traces are shown superimposed; RHC

stores and slightly reduced CCH-induced Ca^{2+} influx, when examined at either maximal (Fig. 2*C*) or sub-maximal (Fig. 2*D*) concentrations of CCh. Thus, as seen with OAG, RHC activated TRPC6 whole-cell currents, but did not increase Ca^{2+} influx as monitored by fura-2 fluorescence.

Effect of U73122 and U73343

U73122, an inhibitor of PLC, has previously been shown to block agonist-induced changes in $[Ca^{2+}]_i$ in most cell types (Bleasdale *et al.* 1990; Smith *et al.* 1990; Thompson *et al.* 1991). Furthermore, previous studies have shown that activation of TRPC6 by receptor stimulation is also blocked by U73122 (Hofmann *et al.* 1999; Inoue *et al.* 2001). U73343, a less active analogue with little or no effect on PLC (Smith *et al.* 1990; Bleasdale *et al.* 1990), is commonly used as a negative control. As expected, U73122 blocked both the CCh-induced release of Ca^{2+} from internal stores in the TRPC6-expressing cells, and the subsequent Ca^{2+} influx observed upon re-admission of Ca^{2+} to the extracellular buffer (Fig. 3*E*). U73343 had no significant effect on either the release of Ca^{2+} from internal stores or on Ca^{2+} influx following re-admission of Ca^{2+}. Much to our surprise, both U73122 and U73343 blocked the CCh-induced increase in TRPC6 currents (Fig. 3*A*–*D*). These compounds were effective when added either before (Fig. 3*C* and *D*) or after CCh (Fig. 3*A* and *B*). Furthermore, the inhibition seen when either U73122 or U73343 was added after activation of TRPC6, was rapid and occurred without delay suggesting a direct, membrane-delimited effect on the TRPC6 channels. As both U73122 and U73343 block the channel, the effect must, at least in part, be independent of PLC. From these experiments it was again clear that the effects observed by whole-cell recording of TRPC6 current were different from those obtained using the fura-2 assay as an indicator of channel activity.

Effect of Na^+

As noted above, all of the fura-2 experiments presented thus far were performed in Ca^{2+}-free–high-K^+ buffer to keep the membrane potential near zero. As previous studies have shown that store-operated and receptor-initiated Ca^{2+} entry is greatly attenuated by depolarization (Schilling, 1989; Schilling *et al.* 1989, 1992), it seemed possible that the failure to observe an increase in $[Ca^{2+}]_i$ in response to OAG may reflect limited Ca^{2+} permeability of TRPC6 channels under depolarized conditions. To test this hypothesis, the fura-2 experiments were repeated in normal HBS. As seen in Fig. 4*A*, addition of OAG had no effect on basal $[Ca^{2+}]_i$ under this condition and the subsequent Ca^{2+} influx component was essentially identical to basal Ca^{2+} influx recorded in the absence of OAG. However, when OAG was added to the cells in the continuous presence of extracellular Ca^{2+}, a small, transient increase in $[Ca^{2+}]_i$ of ~30 nM was observed. A similar increase in $[Ca^{2+}]_i$ was not seen in either wild-type HEK 293 cells or in lacZ-transfected control cells (data not shown). Thus the small increase in $[Ca^{2+}]_i$ is related to TRPC6 expression. When the TRPC6-expressing cells were challenged with OAG in high-K^+ buffer containing 2 mM Ca^{2+}, the change in $[Ca^{2+}]_i$ (~15 nM) was barely detectable (Fig. 4*B*). However, the OAG response was increased in high-K^+ buffer by elevating the extracellular Ca^{2+} to 10 mM (increase $[Ca^{2+}]_i$ of ~50 nM). Overall, these results suggest that activation of TRPC6 current by OAG produces a small increase in $[Ca^{2+}]_i$ in HEK 293 cells under normal ionic conditions, but the response is greatly reduced by holding the membrane potential near zero with high-K^+ buffer; that is, depolarization inhibits Ca^{2+} influx via TRPC6 current.

Evaluation of the Ca^{2+} permeability of TRPC6

The rather modest increase in $[Ca^{2+}]_i$ (<50 nM) induced by OAG under normal ionic conditions may reflect: (1) low permeability of TRPC6 for Ca^{2+} relative to Na^+; (2) a TRPC6 current-induced depolarization; or (3) a combination of both effects. To evaluate the permeability of TRPC6 for Ca^{2+}, we measured TRPC6 currents using extracellular solutions in which the Na^+ and K^+ were replaced by the large, impermeable cation, NMDG. Extracellular Ca^{2+} was then varied from 0.02 to 20 mM. *I–V* relationships from a representative TRPC6-expressing HEK 293 cell under each ionic condition are shown in Fig. 5*A* and on an expanded scale in Fig. 5*C*. Currents were initially activated by OAG in normal Na^+-containing Ringer solution (Fig. 5*A* and *C*). Under this condition, the currents reversed at −7 mV and exhibited the double rectification indicative of TRPC6. In NMDG-containing solution with 0.02 mM Ca^{2+}, the inward current was substantially attenuated and the reversal potential was shifted to −82 mV. Although the currents shown in Fig. 5 were not leak-subtracted, the small inward current seen under this condition reflects, at least in part, a slight permeability of TRPC6 current for NMDG (see below), a characteristic that has been noted for another monovalent cation channel

or CCh were added as indicated to the right of each trace. RHC (50 μM) was added to the cuvette at 50 s, CCh (100 μM) was added at 100 s, and Ca^{2+} (10 mM) was added in each case at 300 s. *D*, same as in *C* except 1 μM CCh was added at the time indicated. Curves represent mean values of three independent experiments; symbols represent mean ± S.E.M. values at selected time points.

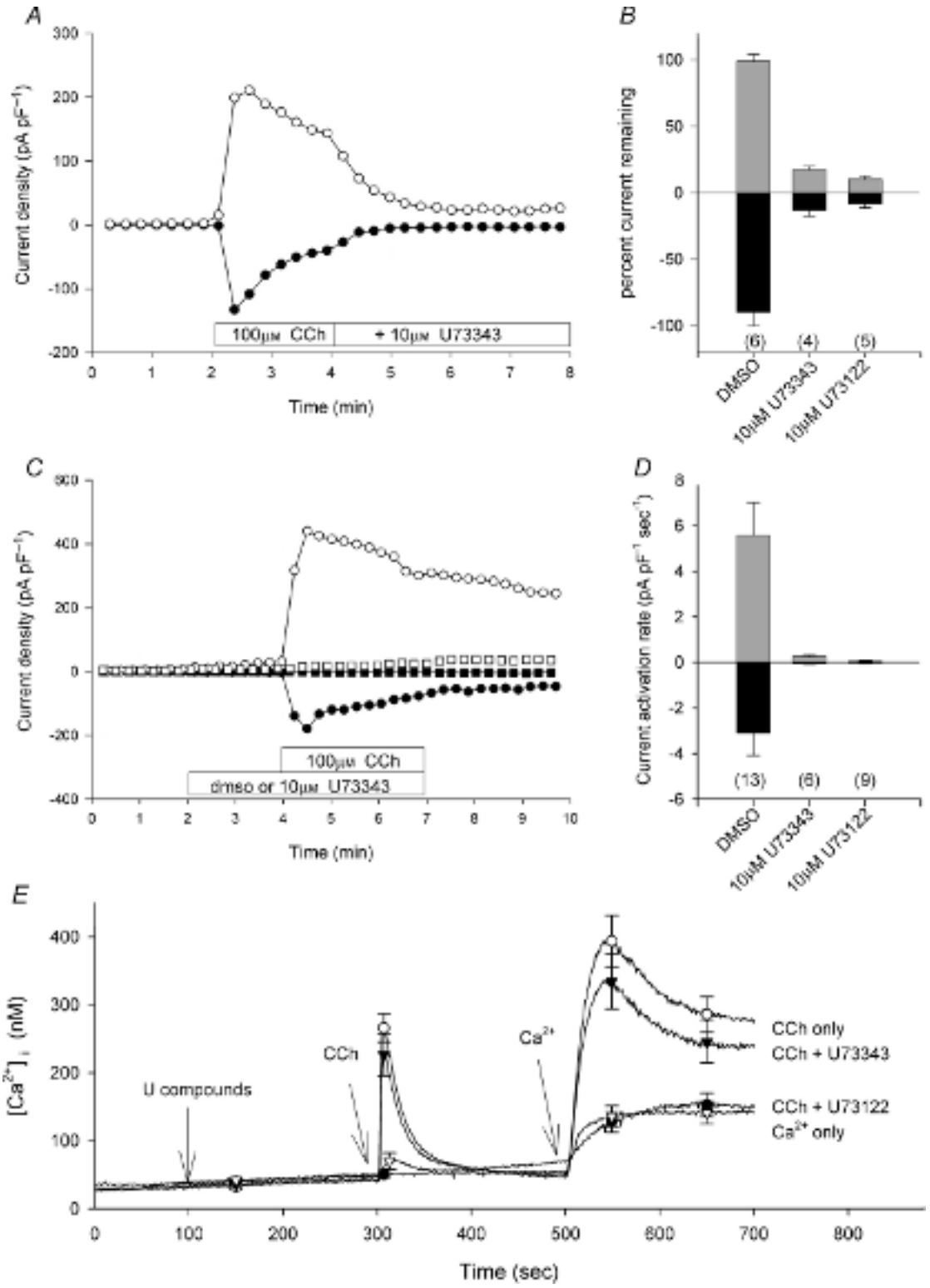

Figure 3. Blockade of TRPC6 by U73122 and U73343

A, whole-cell membrane currents were recorded in TRPC6-expressing HEK 293 cells as described in the legend to Fig. 1. At the time indicated by the horizontal bar, the bath solution was changed to one containing CCh (100 μM). Next, 2 min after addition of CCh, the solution was changed to one containing CCh plus U73343 (10 μM). *B*, mean ± S.E.M. outward (upward bars) and inward (downward bars) current remaining 3 min after the addition of either DMSO (control), U73343 or U73122 as shown in *A*. Numbers in parentheses indicated the number of cells tested under each condition. *C* and *D*, same as *A* and *B*, but with DMSO (circles) or U73343 (squares) added

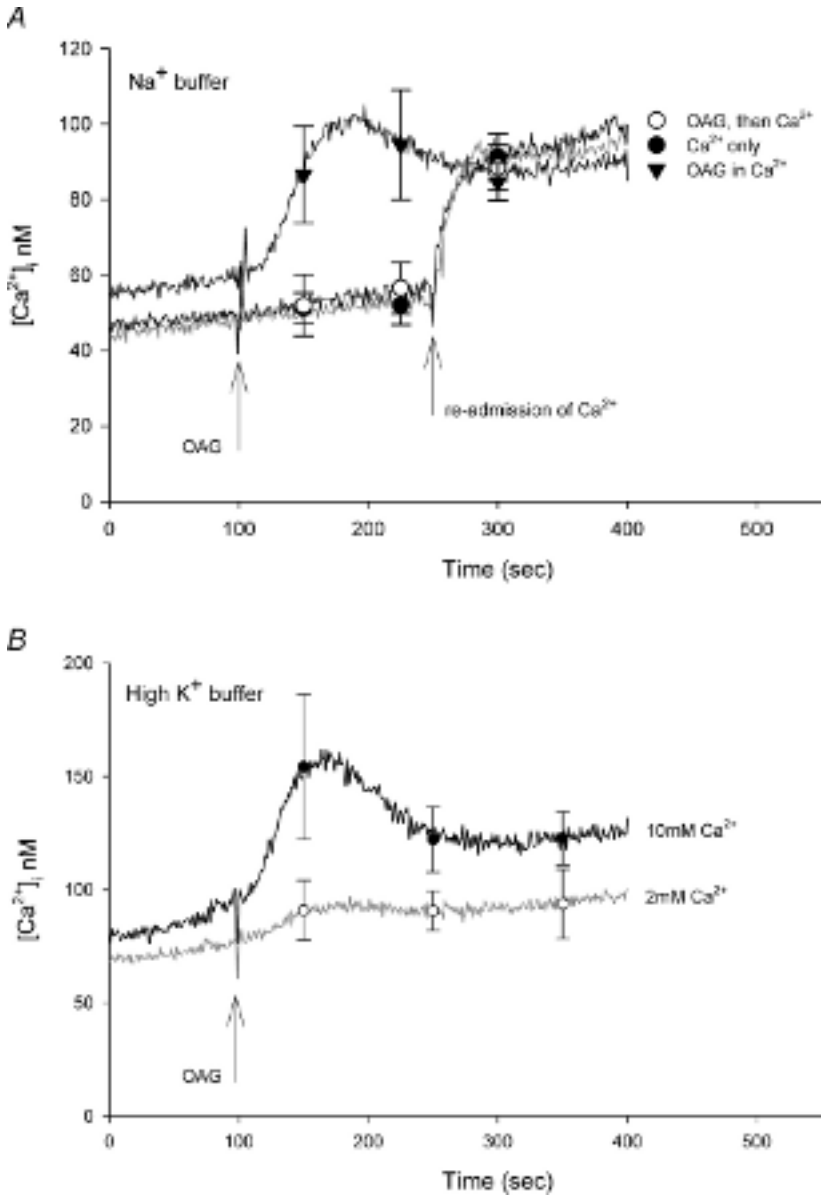

Figure 4. Effect of OAG in the presence of extracellular Ca^{2+}
A, fura-2-loaded HEK 293 cells stably expressing TRPC6 channels were suspended in either normal Na^+-containing HBS (▼) or Ca^{2+}-free–high-K^+ HBS (○ and ●). OAG (100 μM) was added to the cuvette at the time indicated by the arrow in the absence (○) or presence (▼) of 2 mM Ca^{2+}. One trace shows the addition of Ca^{2+} alone at 250 s (●). *B*, fura-2-loaded HEK 293 cells stably expressing TRPC6 channels were suspended in high-K^+ HBS containing either 2 or 10 mM Ca^{2+} as indicated. Curves represent mean values of three independent experiments; symbols represent mean ± S.E.M. values at selected time points.

(Artigas & Gadsby, 2004). In NMDG-containing solution with 2 mM Ca^{2+}, the reversal potential was −56 mV, and outward current was reduced relative to that observed in 0.02 mM Ca^{2+}, but there was little change in inward current amplitude. In NMDG-containing solution with 20 mM Ca^{2+}, the reversal potential was shifted to −24 mV and outward current was further reduced, again without change in inward current. Similar profiles were obtained when TRPC6 currents were measured in HEK 293 cells transiently expressing TRPC6 using the pIRES2-EGFP vector construct as previously described (Estacion *et al.* 2004). Thus, the results are not specific to this clonal cell line.

The insensitivity of inward current to elevations in extracellular $[Ca^{2+}]$, and the concomitant reduction in outward current suggests that Ca^{2+} is acting primarily as a channel blocker rather than a charge carrier. Consistent with this hypothesis, a single-site pore model reproduced the major characteristics of the data set (Fig. 5*B* and *D*). In this model, the binding site within the channel is placed

before CCh. *E*, fura-2-loaded HEK 293 cells stably expressing TRPC6 were suspended in Ca^{2+}-free–high-K^+ HBS. Four traces are shown superimposed; U73122, U73343 and CCh were added as indicated to the right of each trace. U73343 or U73122 (10 μM) were added to the cuvette at 100 s, CCh (100 μM) was added at 300 s, and Ca^{2+} (10 mM) was added in all cases at 500 s. Curves represent mean values of three independent experiments; symbols represent mean ± S.E.M. values at selected time points.

at an electrical distance 85% across the membrane field. If the total electrical potential drop across the membrane thickness is linear, this would place the binding site close to the cytoplasmic surface. The model assumes that Na^+, K^+ and Cs^+ have equal affinity for the binding site of the pore, but that the affinity of the site for Ca^{2+} is approximately two orders of magnitude greater than that for monovalent cations (inset, Fig. 5*B*; see Methods for additional details). Using these basic parameters, the model simulates all of the changes noted upon elevation of extracellular Ca^{2+} from 0.2 to 20 mM including: (1) the rightward shift in reversal potential; (2) the blockade of outward current; and (3) the insensitivity of the inward current. Additionally, the model simulates the dramatic increase in inward current observed in Na^+-containing buffer. However, the model does not reproduce some features seen in the Na^+ data set (compare trace d in Fig. 5*A* and *C* with trace d in Fig. 5*B* and *D*). Specifically, *I–V* relationships generated by the model do not exhibit the slight 'hump' in the current seen around 0 mV or the flattening of inward current seen at potentials more negative than −60 mV. Also, the model predicts that current in Na^+-containing buffer reverses at approximately +5 mV, whereas the actual data traces in the presence of Na^+ reverse at −10 mV. Overall, however, the *I–V* relationships generated by the model are remarkably similar to those derived experimentally. We obtained another set of *I–V* relationships using extracellular buffer in which only the Na^+ was replaced by NMDG; that is,

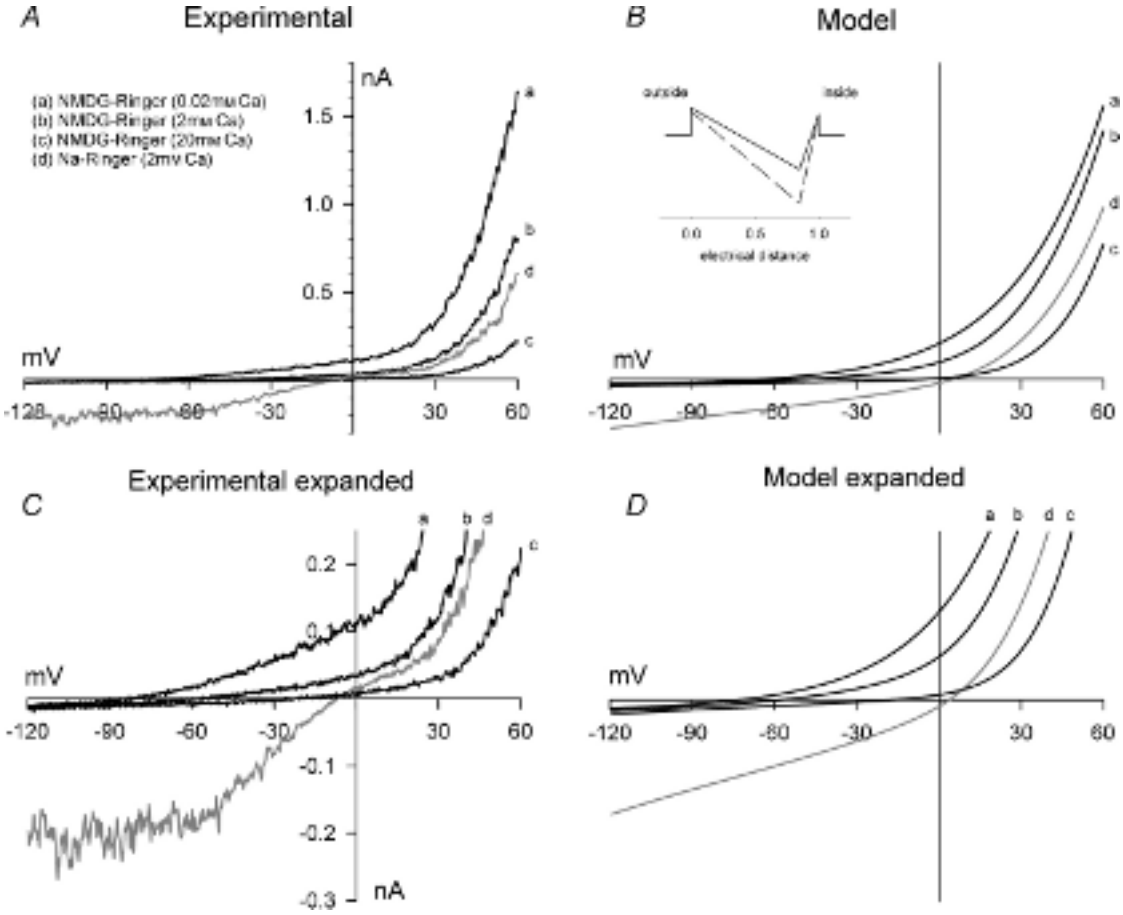

Figure 5. Effect of extracellular Ca^{2+} on whole-cell currents in TRPC6-expressing HEK 293 cells: NMDG buffer

A, currents were recorded as described in the legend to Fig. 1 in HEK 293 cells stably expressing TRPC6. TRPC6 current was activated by superfusion with normal Na^+-containing Ringer solution with 100 μM OAG. A representative *I–V* plot under this condition is shown (d). The extracellular solution was changed to NMDG–$0K^+$ Ringer solution with 0.02 (a), 2 (b) or 20 mM Ca^{2+} (c). *B*, *I–V* relationships predicted by a single-site pore permeation model with the following parameters (see inset): outer and inner barriers were placed at the outer and inner limit of the electric field; the energy well was placed 85% across the electric field; the outer and inner barrier energies for monovalent cations were 4.0 and 3.0 RT units, respectively, and for Ca^{2+} the levels were 3.5 and 3.0 RT units, respectively; and the energy level for the well was −5 and −10 RT units for monovalent cations and Ca^{2+}, respectively. The simulated *I–V* plots are shown for the experimental ionic conditions shown in *A*. *C* and *D*, same as *A* and *B* with an expanded current scale to better visualize the reversal potentials under each condition.

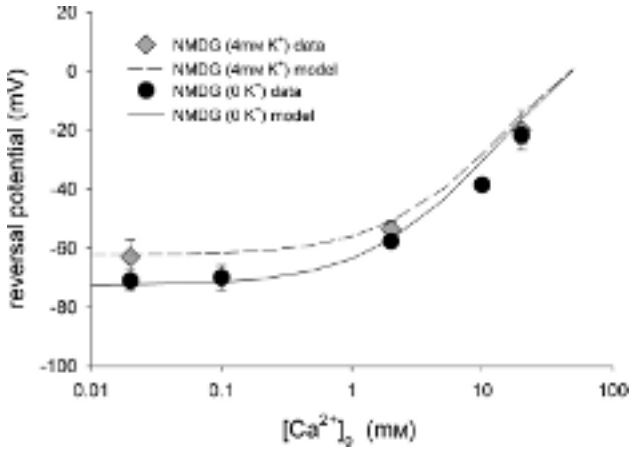

Figure 6. Effect of extracellular Ca^{2+} on reversal potential
The reversal potentials for TRPC6 currents recorded in NMDG-containing solution with either 0 (●) or 4 mM K^+ (◆) as in Fig. 5 are plotted as a function of extracellular Ca^{2+} concentration ($n = 3$–17 for each data point). The lines drawn are the values predicted from the single-site pore model under each ionic condition.

4 mM K^+ was present in the extracellular buffer (Fig. 1 of Supplemental material, available on-line). Using model parameters identical to those shown in Fig. 5, the model was again able to reproduce reversal potential shifts and account for the presence of K^+. The mean (± S.E.M.) reversal potentials for several experiments are plotted in Fig. 6 for each Ca^{2+} concentration tested in either the presence or absence of K^+. The lines shown in Fig. 6 represent the reversal potentials predicted by the model as a function of extracellular Ca^{2+} concentration and the symbols are the actual reversal potentials measured under each condition. Again there is excellent agreement between the experimental and the predicted values. It is important to note that calculation of the relative permeability of TRPC6 for Ca^{2+} *versus* monovalent cations based on the experimentally determined reversal potentials in 2 or 20 mM Ca^{2+} yields values of 1.23 and 1.06, respectively. Thus, although the relative permeability of TRPC6 for Ca^{2+} *versus*, in this

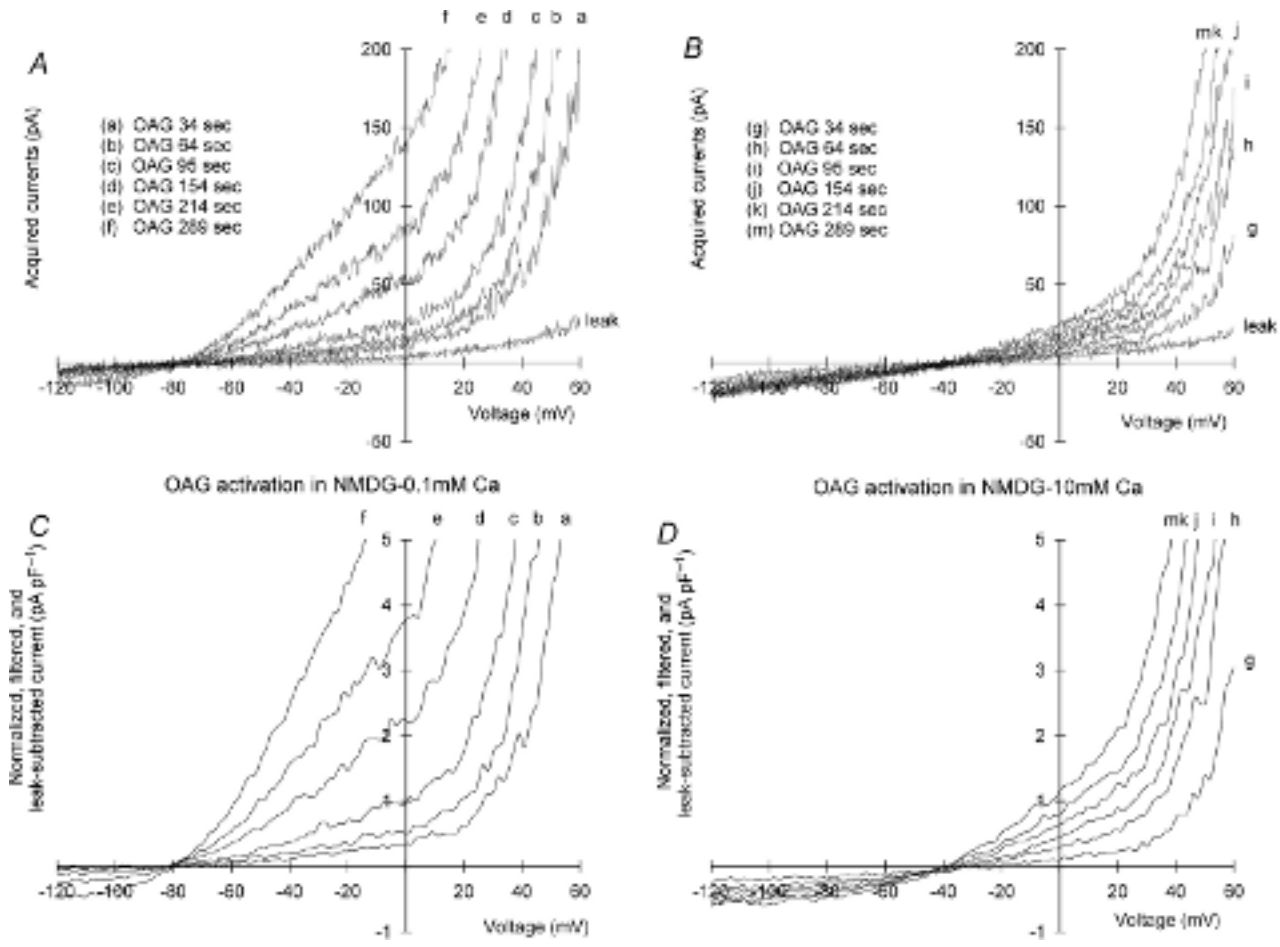

Figure 7. Activation of TRPC6 current in low- or high-Ca^{2+} buffer
A and B, currents were recorded as described in the legend to Fig. 1 in HEK 293 cells stably expressing TRPC6. TRPC6 current was activated by superfusion with NMDG–0K^+ Ringer solution containing 0.1 (*A*) or 10 mM Ca^{2+} (*B*) plus 100 μM OAG. *I–V* curves are shown before OAG (leak) and as a function of time after addition of OAG (see inset to *A* and *B*). *C* and *D*, currents from *A* and *B* were leak-subtracted, normalized to capacitance, and filtered at 200 Hz.

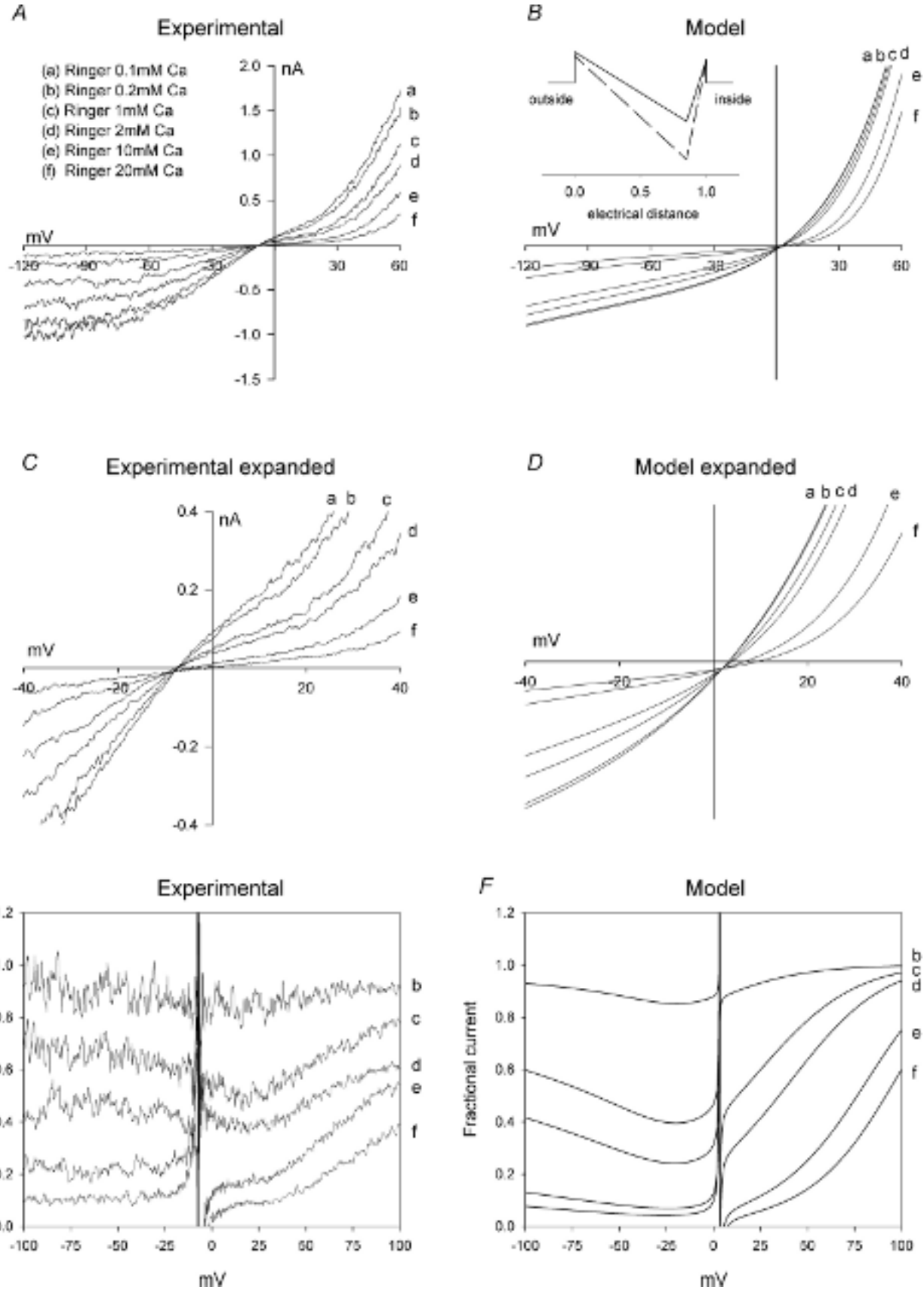

case, Cs^+ remains essentially constant at 1 as extracellular Ca^{2+} concentration is increased, the conductance is greatly reduced due to channel blockade.

As mentioned above, a small inward current was observed in NMDG-containing buffer with 0.02 mM Ca^{2+}, suggesting that TRPC6 may have a slight permeability to NMDG. However, in these experiments, the TRPC6 currents were activated in Na^+-containing buffer prior to solution change. It is difficult using this protocol to determine the contribution of 'leak' currents to the total current recorded under each ionic condition. To obtain a better estimate of both the leak current and Ca^{2+} permeability, we monitored the activation of TRPC6 current by OAG while the cell was bathed in NMDG-containing buffer with either 0.1 (Fig. 7*A* and *C*) or 10 mM Ca^{2+} (Fig. 7*B* and *D*). Under this condition, voltage ramps in the absence of OAG reflect leak currents and subsequent voltage ramps in the presence of OAG reflect the time-dependent activation of TRPC6. In the low-Ca^{2+} solution, a small inward TRPC6 current component activated in a time-dependent fashion following addition of OAG, suggesting that TRPC6 has a small, but detectable permeability to NMDG. The current reversed near −80 mV and the normalized current amplitude recorded 30 mV negative to the reversal potential was −0.40 pA pF^{-1} (Fig. 7*C*). Inward TRPC6 currents were also activated in NMDG buffer containing 10 mM Ca^{2+}. The currents reversed near −40 mV and achieved an amplitude of −0.45 pA pF^{-1} recorded 30 mV negative to the reversal potential (Fig. 7*D*). Thus, despite the fact that extracellular Ca^{2+} concentration differed by 10-fold, inward TRPC6 current was the same. However, the single-site pore model predicts that the majority of inward current observed in the presence of 0.1 mM Ca^{2+} is carried by NMDG, whereas in 10 mM Ca^{2+}, essentially all the current observed is carried by Ca^{2+}. Thus, the conductance of TRPC6 for Ca^{2+} is low, but predicted to be finite. We repeated this series of experiments with Ba^{2+} (Fig. 2 in Supplemental material, available on-line). The profile obtained was essentially the same as with Ca^{2+}, with the exception that Ba^{2+} produced less block of outward current.

With Na^+ and K^+ in the extracellular buffer, the model predicts that inward current will be inhibited by extracellular Ca^{2+} and that little change in reversal potential will be observed as the Ca^{2+} concentration is varied (Fig. 8*B* and *D*). To test this hypothesis, extracellular Ca^{2+} concentration in normal Na^+ Ringer solution was varied from 0.1 to 20 mM. The *I–V* relationships from a representative cell are shown in Fig. 8*A* and *C*. Once again, the experimental data set is very similar to that predicted by the single-site pore model with parameters exactly the same as those used to describe the previous data sets. To determine whether channel blockade by Ca^{2+} is voltage sensitive, the current observed at each extracellular Ca^{2+} concentration (i.e. 0.2–20 mM) was divided by that observed at 0.1 mM Ca^{2+} and the fractional current was plotted as a function of membrane potential (Fig. 8*E*). Over the negative voltage range, membrane potential has little effect on channel blockade by Ca^{2+}. However, at 1 and 2 mM extracellular Ca^{2+} concentration, the block increases slightly as the potential approaches zero. At positive potentials, there is clear relief of blockade as the voltage is increased from 0 to +100 mV. Again, the predictions from the single-site pore model are remarkably similar to the experimentally derived profiles (Fig. 8*F*). To estimate the contribution of Ca^{2+} flux via TRPC6 to the total inward current in the presence of extracellular Na^+ and K^+, the individual net ion fluxes predicted by the model in Fig. 8 for the condition in the presence of 2 mM Ca^{2+} were plotted as a function of potential (Fig. 3 of Supplemental material, available on-line). At −100 mV, inward monovalent current, which primarily reflects Na^+ influx, was −116 pA. In contrast, the magnitude of Ca^{2+} current at −100 mV was predicted to be −4.6 pA. Thus, the model predicts that the proportion of inward TRPC6 current carried by Na^+ *versus* Ca^{2+} under normal extracellular ionic conditions is approximately 25 : 1.

Effect of membrane potential

The results of the experiments presented thus far suggest that TRPC6 has a low inherent Ca^{2+} conductance and that

Figure 8. Effect of extracellular Ca^{2+} on whole-cell currents in TRPC6-expressing HEK 293 cells: normal Na^+ buffer

A, currents were recorded as described in the legend to Fig. 1 in HEK 293 cells stably expressing TRPC6. TRPC6 current was activated by superfusion with normal Na^+-containing Ringer solution containing 100 μM OAG. A representative *I–V* curve under this condition is shown (d). The extracellular solution was changed to Na^+-containing Ringer solution with various Ca^{2+} concentrations (inset). *B*, *I–V* relationships predicted by the single-site pore permeation model with the parameter set given in the legend to Fig. 5. The simulated *I–V* curves are shown for the experimental ionic conditions shown in *A*. *C and D*, same as *A* and *B* with an expanded current scale to better visualize the reversal potentials under each condition. *E* and *F*, to determine the voltage-dependence of the block by Ca^{2+}, current traces in 0.2–20 mM Ca^{2+} were normalized to the values observed in the presence of 0.1 mM Ca^{2+}. Fractional current is shown as a function of membrane potential for both the experimental and model-derived data sets as indicated.

depolarization further attenuates Ca^{2+} entry via TRPC6. However, it might be possible to observe Ca^{2+} entry via TRPC6 if the membrane potential is held sufficiently negative. To test this hypothesis, cells were loaded with fura-2 and then subjected to whole-cell voltage clamp using the perforated-patch technique as described in the Methods. Fluorescence images were acquired from the patched cell and from all unpatched cells in the field of view. A representative experiment is shown in Fig. 9. Addition of OAG (100 μM) in Na^+-containing Ringer solution with 0.02 mM extracellular Ca^{2+} had no effect on $[Ca^{2+}]_i$ but clearly caused an increase in whole-cell current with an *I–V* relationship characteristic of TRPC6 current (Fig. 9, inset). At a holding potential of −50 mV, addition of 2 mM Ca^{2+} in the continuous presence of OAG caused an increase in $[Ca^{2+}]_i$ that was substantially greater than that observed in the unpatched cells. Changing holding potential to +50 mV caused a decrease in $[Ca^{2+}]_i$, whereas changing the holding potential to −80 mV caused a further increase in $[Ca^{2+}]_i$. Thus, Ca^{2+} influx via TRPC6 appears to follow the electrochemical driving force imposed by the holding potential. This basic experiment was repeated four times in Na^+-containing Ringer solution and the results from the patched cells held at −50 mV are shown in Fig. 10*A* and from the unpatched cells in Fig. 10*C*. Although the exact membrane potential of the unpatched cells is unknown, the reversal potential for whole-cell TRPC6 currents under this condition is approximately −7 mV (see Fig. 5). Thus, if TRPC6 current dominates the whole-cell conductance, the membrane potential of the unpatched cells should approach −7 mV. Upon increasing the extracellular Ca^{2+} concentration in the presence of OAG, $[Ca^{2+}]_i$ increased in the patched cells to 131 ± 34 nM, whereas $[Ca^{2+}]_i$ increased in the unpatched cells to only 41 ± 2 nM. In order to increase the driving force for Ca^{2+} entry in the unpatched cells, this experiment was repeated in NMDG-containing Ringer solution. Under this ionic condition, the reversal potential for the whole-cell TRPC6 current is approximately −56 mV (see Fig. 5). As seen in Fig. 10*D*, $[Ca^{2+}]_i$ increased to 58 ± 5 nM in the unpatched cells, whereas in the patched cells held at −50 mV the value was 135 ± 28 nM. Thus, following activation of TRPC6 current by OAG, the membrane potential of the unpatched cells in the presence of NMDG is more negative than in the presence of Na^+, but less negative than −50 mV. In order to obtain a better estimate of basal Ca^{2+} influx in these experiments, the cells were first perfused with Ca^{2+} in the absence of OAG and then re-perfused with Ca^{2+} in the presence of OAG (Fig. 11). In Na^+-containing Ringer solution, the change in $[Ca^{2+}]_i$ upon addition of Ca^{2+} to the bath was the same in the presence or absence of OAG. However, in NMDG-containing Ringer solution,

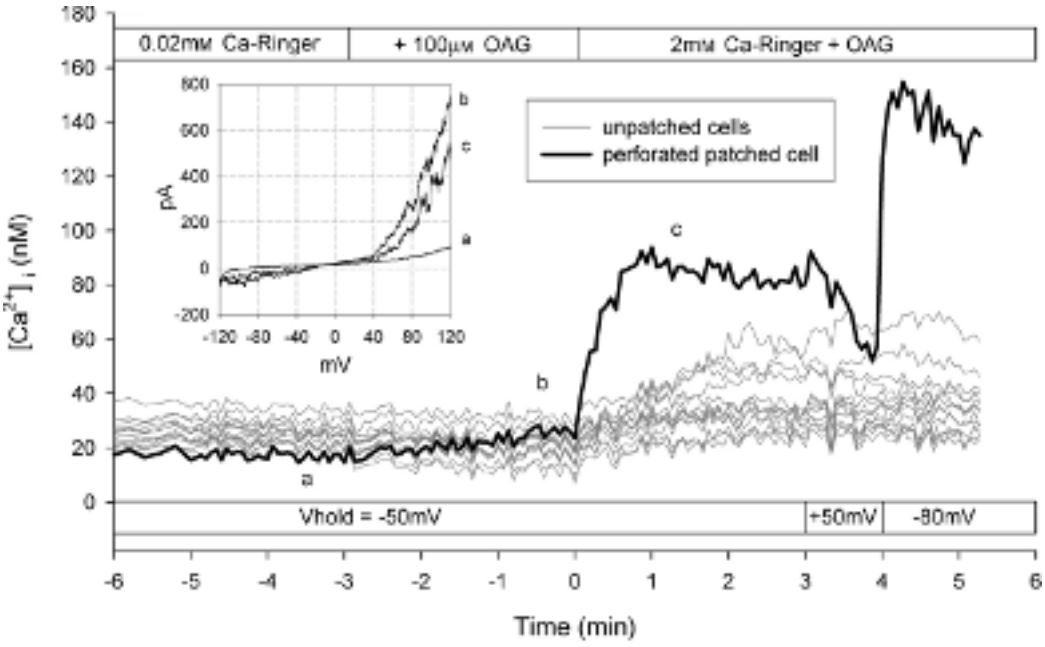

Figure 9. Simultaneous recording of membrane current and fura-2 fluorescence using the perforated-patch technique and optical imaging
HEK 293 cells stably expressing TRPC6 were loaded with fura-2 using the AM form. Whole-cell membrane currents were recorded in one cell using the perforated-patch technique and $[Ca^{2+}]_i$ was determined as a function of time in all cells within the field of view as described in the Methods. The inset shows the *I–V* relationship at the indicated time points (a–c). Upper horizontal bar indicates solution changes, whereas the lower bar indicates holding potential of the cell subjected to voltage clamp. $[Ca^{2+}]_i$ is shown for the patched cell (black trace) and for each individual unpatched cell (grey traces). Result shown is from a single coverslip.

an OAG-induced increase in $[Ca^{2+}]_i$ was clearly seen. Taken together, the results suggest that although Ca^{2+} conductance of TRPC6 is low relative to monovalent cation conductance, an increase in $[Ca^{2+}]_i$ can be observed if membrane potentials are held sufficiently negative.

Discussion

TRPC channels are thought to be Ca^{2+}-permeable cation channels responsible for receptor-mediated Ca^{2+} entry in a variety of excitable and non-excitable cells. Using fluorescence techniques, three independent groups have reported that over-expression of TRPC6 in either COS (Boulay *et al.* 1997; Zhang & Saffen, 2001), CHO (Hofmann *et al.* 1999) or HEK 293 cells (Lessard *et al.* 2005) is associated with an increase in Ca^{2+} influx in response to receptor stimulation and OAG. In contrast, increasing extracellular Ca^{2+} concentration in Na^+-containing buffers during the recording of TRPC6 currents by voltage-clamp technique caused a reduction in both inward and outward current, suggestive of channel blockade (Inoue *et al.* 2001; Shi *et al.* 2004). A similar result has been reported for TRPC7 channels expressed in HEK 293 cells (Shi *et al.* 2004), and for TRPC3 channels over-expressed in endothelial cells, where an increase in

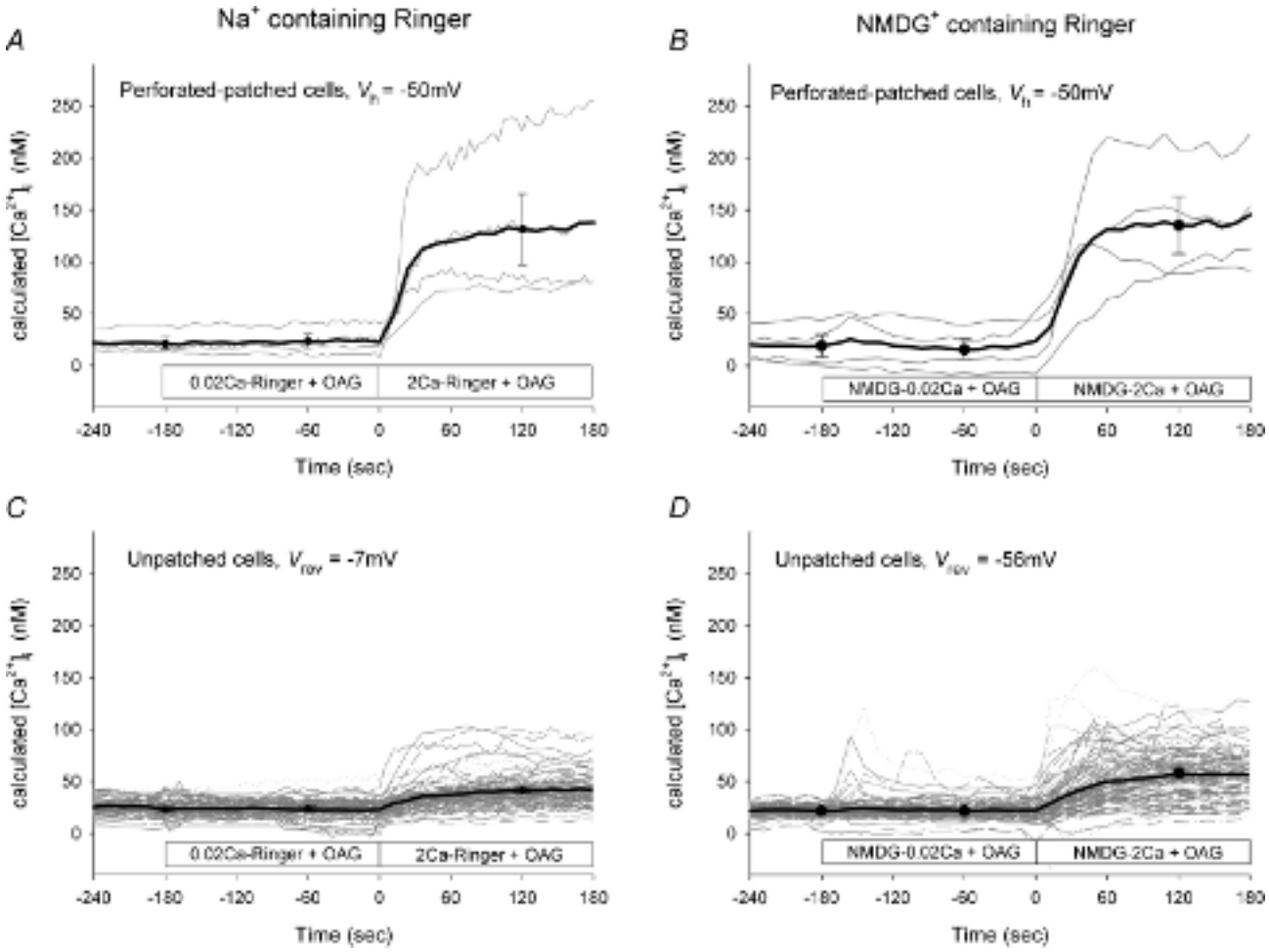

Figure 10. Effect of membrane potential on $[Ca^{2+}]_i$ in TRPC6-expressing HEK 293 cells
$[Ca^{2+}]_i$ was determined as described in the legend to Fig. 9 in both patched cells (*A* and *B*) and unpatched cells (*C* and *D*) in the field of view. Patched cells ($n = 4$) were held at −50 mV throughout the experiment. Horizontal bar indicates the solution changes. Panels on the left were recorded in normal Na^+-containing Ringer solution, whereas those on the right were obtained in NMDG-containing Ringer solution. Black lines in *A* and *B* represent mean values of four cells; symbols represent mean ± S.E.M. values at selected time points. Black lines in *C* and *D* represent mean values of 9–10 independent experiments (i.e. coverslips); symbols represent mean ± S.E.M. values at selected time points. Individual cells are shown in grey (*C*, $n = 103$ cells; *D*, $n = 112$ cells). V_{rev} indicates the value of the TRPC6 current reversal potentials from Fig. 5 recorded in either Na^+ or $NMDG^+$. V_h is the holding potential.

Ca^{2+} concentration from 0 to 1.5 mM significantly reduced TRPC3 currents (Kamouchi *et al.* 1999). Likewise, native currents in A7r5 smooth muscle cells, which appear to reflect the activity of endogenous TRPC6 channels, are reversibly increased by reducing the extracellular Ca^{2+} concentration from 2 mM to 50 μM and greatly attenuated by increasing the concentration to 10 or 100 mM (Jung *et al.* 2002). Thus, the actual permeability of TRPC6 channels for Ca^{2+} in the presence of normal Na^+ remains unclear. In the present study, we compared Ca^{2+} influx as estimated by fura-2 fluorescence to changes in membrane current measured electrophysiologically in HEK 293 cells stably expressing human TRPC6. Stimulation of muscarinic receptors with CCh resulted in a robust activation of TRPC6 currents and caused a dramatic increase in $[Ca^{2+}]_i$. However, three lines of evidence suggest that this rise in $[Ca^{2+}]_i$ is unrelated to TRPC6. First, TRPC6 currents were activated by OAG, but OAG had no effect on Ca^{2+} influx as estimated by the Ca^{2+} re-admission protocol. Second, TRPC6 currents were activated by RHC, an inhibitor of DAG lipase. Again, however, RHC had no effect on basal or carbachol-induced Ca^{2+} influx, even when examined at submaximal concentrations. Third, as expected, TRPC6 currents were blocked by U73122, an inhibitor of PLC. It was surprising to find that TRPC6 currents were also blocked by the inactive analogue, U73343. In contrast, U73122 blocked carbachol-induced Ca^{2+} influx in TRPC6-expressing cells, whereas U73343 had little or no effect. Together these results suggest that activation of TRPC6 current has little impact on $[Ca^{2+}]_i$, and that the carbachol-induced increase in $[Ca^{2+}]_i$ primarily reflects activation of endogenous Ca^{2+} entry pathways present in this HEK 293 cell line. However, these fura-2 experiments were performed in high-K^+ buffer to hold the membrane potential near zero. A small, OAG-induced increase in $[Ca^{2+}]_i$ was observed in normal Na^+ solution and in high-K^+ buffer containing 10 mM Ca^{2+}. These results suggest that depolarization inhibits Ca^{2+} entry via TRPC6. Indeed, using the perforated-patch technique, OAG-induced changes in Ca^{2+} influx via TRPC6 could be readily observed if the cell was clamped to −50 mV while simultaneously recording fura-2 fluorescence. Likewise, Ca^{2+} influx was observed if Na^+ in the extracellular solution was replaced by NMDG, an ionic condition that limits the depolarizing influence of TRPC6 channel activity. Thus, a Ca^{2+} influx via TRPC6 sufficient to increase $[Ca^{2+}]_i$, requires a rather substantial negative membrane potential. It has been known for some time that both receptor-mediated and store-operated Ca^{2+} entry are greatly attenuated by depolarization (Schilling, 1989; Schilling *et al.* 1989; Schilling *et al.* 1992), but for TRPC6 channels the effect of depolarization appears to be greater

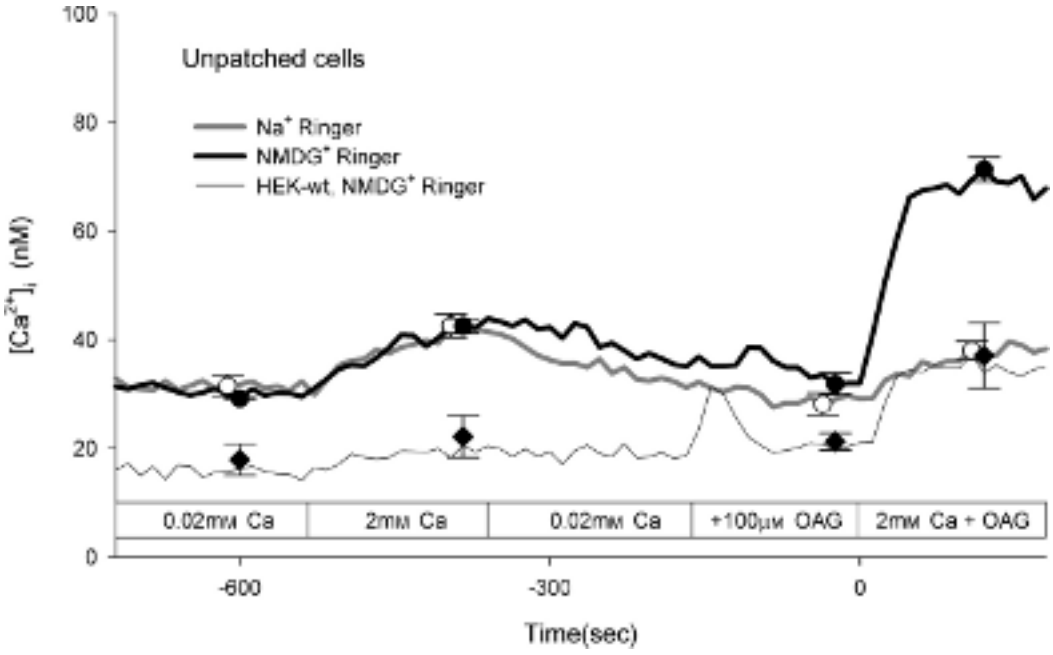

Figure 11. OAG has no effect on $[Ca^{2+}]_i$ in normal Na^+-containing Ringer solution
$[Ca^{2+}]_i$ was determined as described in the legend to Fig. 9 on HEK 293 cells stably expressing TRPC6 channels perfused with Na^+- (●) or NMDG-containing Ringer solution (○, see inset). The horizontal bar indicates the solution changes. For comparison, the same experiment was performed on wild-type HEK 293 cells perfused with NMDG-containing Ringer solution (♦). Curves represent mean values of three independent experiments; symbols represent mean ± S.E.M. values at selected time points. For clarity, individual cells under each condition (51, 42 and 75 cells) are not shown.

than would be predicted based on changes in driving force alone. This result, however, is consistent with the *I–V* relationship which shows a dramatic reduction in current amplitude as membrane potential moves from −50 to +40 mV, giving rise to the characteristic plateau in TRPC6 current seen around 0 mV. Recent studies have suggested that this may reflect blockade by intracellular Mg^{2+} (Obukhov & Nowycky, 2005).

Although it is clear that activation of TRPC6 current by OAG can increase $[Ca^{2+}]_i$, the magnitude of the response was rather modest when compared to that observed following muscarinic receptor stimulation. This rather surprising result prompted us to examine the Ca^{2+} permeability of TRPC6 channels in greater detail using electrophysiological approaches. In the first protocol, TRPC6 channels were activated by OAG in buffer containing normal concentrations of Na^+ and K^+. The extracellular solution was then changed to one containing NMDG and various concentrations of Ca^{2+}. If the channels were permeable to Ca^{2+}, we anticipated rightward shifts in reversal potential and increases in inward current as Ca^{2+} was increased. Although the reversal potentials shifted as expected (i.e. to the right), inward current did not appreciably change and outward current was dramatically reduced as the Ca^{2+} concentration was increased in the extracellular buffer. In the second protocol, the extracellular solution was changed to the NMDG-containing solution with a fixed concentration of Ca^{2+} before activation of the channels with OAG. This allowed for a good estimate of leak current before activation of TRPC6 channels. Again, the results showed that inward currents were little affected by activation of TRPC6 under conditions that were expected to yield large Ca^{2+} currents. Together the results suggest that Ca^{2+} acts more as a TRPC6 channel blocker than a charge carrier. To estimate the contribution of Ca^{2+} to total inward current in the presence of normal Na^+ and K^+ levels, we simulated the experimental conditions using a single-site pore model in which the binding site of the pore was placed close to the cytoplasmic membrane surface and the affinity of the binding site for Ca^{2+} was approximately two orders of magnitude greater than that for monovalent cations. Although permeation in this channel is likely to be more complex, the simple single-site pore model reproduced the major features of the TRPC6 currents recorded under various ionic conditions and clearly supports the conclusion that TRPC6 channels have a limited Ca^{2+} permeability. Under physiological ionic conditions, the model predicts that TRPC6 channels are primarily monovalent cation channels. If activation is sustained, this could lead to a gain of Na^+ and loss of K^+ by the cell. This could explain our recent observation that TRPC6 channels physically associates with the Na^+–K^+- ATPase/pump in kidney and brain, and in the plasmalemma of the TRPC6-expressing HEK 293 cell line used in the present study (Goel *et al.* 2005). As suggested for TRPC3 (Rosker *et al.* 2004), alteration in the Na^+ gradient could also lead to Ca^{2+} entry via the Na^+–Ca^{2+} exchanger or may enhance Ca^{2+} signalling events in restricted subplasmalemmal compartments (Arnon *et al.* 2000). It is interesting that TRPC6 current-induced membrane depolarization and the subsequent activation of voltage-gated Ca^{2+} channels has been implicated in myogenic contraction of arterial smooth muscle cells (Welsh *et al.* 2002). In contrast, TRPC3 channels mediate depolarization and contraction of arterial smooth muscle in response to receptor stimulation (Reading *et al.* 2005). In a recent study using A7r5 smooth muscle cells, activation of endogenous TRPC6 channels by OAG causes an increase in $[Ca^{2+}]_i$ that is blocked by nimodipine, suggesting that the rise in $[Ca^{2+}]_i$ reflects a TRPC6-induced depolarization which in turn activates voltage-gated Ca^{2+} channels (Soboloff *et al.* 2005).

Taken together, the results of the present study suggest that TRPC6 channels play a dual role in signal transduction. In cells with high input resistance, the primary effect of TRPC6 activation will be depolarization, which limits Ca^{2+} entry via TRPC6 channels, but may facilitate a rapid burst of Ca^{2+} entry via voltage-gated Ca^{2+} channels if present. In cells with, for example, a large inward-rectifier or Ca^{2+}-activated K^+ channel current to hold the membrane potential negative, receptor-mediated activation of TRPC6 will directly serve as a sustained Ca^{2+} influx pathway. Thus, TRPC6 channels can perform a dual signalling role to either depolarize the cell and rapidly deliver Ca^{2+} or provide a more sustained change in $[Ca^{2+}]_i$ depending on the particular needs of the cell and the complement of other channel types.

References

Arnon A, Hamlyn JM & Blaustein MP (2000). Ouabain augments Ca^{2+} transients in arterial smooth muscle without raising cytosolic Na^+. *Am J Physiol Heart Circ Physiol* **279**, H679–H691.

Artigas P & Gadsby DC (2004). Large diameter of palytoxin-induced Na/K pump channels and modulation of palytoxin interaction by Na/K pump ligands. *J Gen Physiol* **123**, 357–376.

Bandyopadhyay BC, Swaim WD, Liu X, Redman R, Patterson RL & Ambudkar IS (2005). Apical localization of a functional TRPC3/TRPC6-Ca^{2+}-signaling complex in polarized epithelial cells: role in apical Ca^{2+} influx. *J Biol Chem* **280**, 12908–12916.

Bleasdale JE, Thakur NR, Gremban RS, Bundy GL, Fitzpatrick FA, Smith RJ & Bunting S (1990). Selective inhibition of receptor-coupled phospholipase C-dependent processes in human platelets and polymorphonuclear neutorphils. *J Pharmacol Exp Ther* **255**, 756–768.

Boulay G, Zhu X, Peyton M, Hurst R, Stefani E & Birnbaumer L (1997). Cloning and expression of a novel mammalain homolog of Drosophila transient receptor potential (Trp) involved in calcium entry secondary to activation of receptors coupled by G_q class of G protein. *J Biol Chem* **272**, 29672–29680.

Chu X, Tong Q, Cheung JY, Wozney J, Conrad K, Mazack V, Zhang W, Stahl R, Barber DL & Miller BA (2004). Interaction of TRPC2 and TRPC6 in erythropoietin modulation of calcium influx. *J Biol Chem* **279**, 10514–10522.

Clapham DE (2003). TRP channels as cellular sensors. *Nature* **426**, 517–524.

Corteling RL, Li S, Giddings J, Westwick J, Poll C & Hall IP (2004). Expression of transient receptor potential C6 and related transient receptor potential family members in human airway smooth muscle and lung tissue. *Am J Respir Cell Mol Biol* **30**, 145–154.

Dietrich A, Schnitzler MM, Emmel J, Kalwa H, Hofmann T & Gudermann T (2003). N-linked protein glycosylation is a major determinant for basal TRPC3 and TRPC6 channel activity. *J Biol Chem* **278**, 47842–47852.

Estacion M, Applegate MAB, Jones SW, Sinkins WG & Schilling WP (2005). Human TRPC6 forms non-selective cation channels with limited Ca^{2+} permeability. *FASEB J* **19**, A1163.

Estacion M, Li S, Sinkins WG, Gosling M, Bahra P, Poll C, Westwick J & Schilling WP (2004). Activation of human TRPC6 channels by receptor stimulation. *J Biol Chem* **279**, 22047–22056.

Frazier CJ, George EG & Jones SW (2000). Apparent change in ion selectivity caused by changes in intracellular K^+ during whole-cell recording. *Biophys J* **78**, 1872–1880.

Garcia RL & Schilling WP (1997). Differential expression of mammalian Trp homologues across tissues and cell lines. *Biochem Biophys Res Commun* **239**, 279–283.

Goel M, Sinkins WG, Keightley A, Kinter M & Schilling WP (2005). Proteomic analysis of TRPC5- and TRPC6-binding partners reveals interaction with the plasmalemmal Na^+/K^+-ATPase. *Pflugers Arch - Eur J Physiol* **451**, 87–98.

Goel M, Sinkins WG & Schilling WP (2002). Selective association of TRPC channel subunits in rat brain synaptosomes. *J Biol Chem* **277**, 48303–48310.

Grynkiewicz G, Poenie M & Tsien RY (1985). A new generation of Ca^{2+} indicators with improved fluorescence properties. *J Biol Chem* **260**, 3440–3450.

Hassock SR, Zhu MX, Trost C, Flockerzi V & Authi KS (2002). Expression and role of TRPC proteins in human platelets: evidence that TRPC6 forms the store-independent calcium entry channel. *Blood* **100**, 2801–2811.

Hille B (2001). Selective permeability: saturation and binding. In *Ion Channels of Excitable Membrane*. Hille B, pp. 471–502. Sinauer Associates, Inc., Massachusetts.

Hofmann T, Obukhov AG, Schaefer M, Harteneck C, Gudermann T & Schultz G (1999). Direct activation of human TRPC6 and TRPC3 channels by diacylglycerol. *Nature* **397**, 259–263.

Hofmann T, Schaefer M, Schultz G & Gudermann T (2002). Subunit composition of mammalian transient receptor potential channels in living cells. *Proc Natl Acad Sci U S A* **99**, 7461–7466.

Inoue R, Okada T, Onoue H, Hara Y, Shimizu S, Naitoh S, Ito Y & Mori Y (2001). The transient receptor potential protein homologue TRP6 is the essential component of vascular α1-adrenoceptor activated Ca^{2+}-permeable cation channel. *Circ Res* **88**, 325–332.

Jung S, Strotmann R, Schultz G & Plant TD (2002). TRPC6 is a candidate channel involved in receptor stimulated cation currents in A7r5 smooth muscle cells. *Am J Physiol Cell Physiol* **282**, C347–C359.

Kamouchi M, Philipp S, Flockerzi V, Wissenbach U, Mamin A, Raeymaekers L, Eggermont J, Droogmans G & Nilius B (1999). Properties of heterologously expressed hTRP3 channels in bovine pulmonary artery endothelial cells. *J Physiol* **518**, 345–358.

Korn SJ & Horn R (1989). Influence of sodium-calcium exchange on calcium current rundown and the duration of calcium-dependent chloride currents in pituitary cells studied with whole cell and perforated patch recording. *J Gen Physiol* **94**, 789–812.

Lessard CB, Lussier MP, Cayouette S, Bourque G & Boulay G (2005). The overexpression of presenilin2 and Alzheimer's-disease-linked presenilin2 variants influences TRPC6-enhanced Ca^{2+} entry into HEK293 cells. *Cell Signal* **17**, 437–445.

Montell C (2005). The TRP superfamily of cation channels. *Sci STKE*; DOI: 10.1126/stke.2722005re3.

Obukhov AG & Nowycky MC (2005). A cytosolic residue mediates Mg^{2+} block and regulates inward current amplitude of a transient receptor potential channel. *J Neurosci* **25**, 1234–1239.

Okada T, Inoue R, Yamazaki K, Maeda A, Kurosaki T, Yamakuni T, Tanaka I, Shimizu S, Ikenaka K, Imoto K & Mori Y (1999). Molecular and functional characterization of a novel mouse transient receptor potential protein homologue TRP7. *J Biol Chem* **274**, 27359–27370.

Reading SA, Earley S, Waldron BJ, Welsh DG & Brayden JE (2005). TRPC3 mediates pyrimidine receptor-induced depolarization of cerebral arteries. *Am J Physiol Heart Circ Physiol* **288**, H2055–H2061.

Riccio A, Medhurst AD, Mattei C, Kelsell RE, Calver AR, Randall AD, Benham CD & Pannier B (2002). mRNA distribution analysis of human TRPC familly in CNS and peripheral tissues. *Mol Brain Res* **109**, 95–104.

Rosker C, Graziani A, Lukas M, Eder P, Zhu MX, Romanin C & Groschner K (2004). Ca^{2+} signaling by TRPC3 involves Na^+ entry and local coupling to the Na^+/Ca^{2+} exchanger. *J Biol Chem* **279**, 13696–13704.

Schilling WP (1989). Effect of membrane potential on cytosolic calcium of bovine aortic endothelial cells. *Am J Physiol* **257**, H778–H784.

Schilling WP, Cabello OA & Rajan L (1992). Depletion of the inositol 1,4,5-trisphosphate-sensitive intracellular Ca^{2+} store in vascular endothelial cells activates the agonist-sensitive Ca^{2+}-influx pathway. *Biochem J* **284**, 521–530.

Schilling WP, Rajan L & Strobl-Jager E (1989). Characterization of the bradykinin-stimulated calcium influx pathway of cultured vascular endothelial cells: saturability, selectivity and kinetics. *J Biol Chem* **264**, 12838–12848.

Shi J, Mori E, Mori Y, Mori M, Li J, Ito Y & Inoue R (2004). Multiple regulation by calcium of murine homologues of transient receptor potential proteins TRPC6 and TRPC7 expressed in HEK293 cells. *J Physiol* **561**, 415–432.

Smith RJ, Sam LM, Justen JM, Bundy GL, Bala GA & Bleasdale JE (1990). Receptor-coupled signal transduction in human polymorphonuclear neutrophils: Effects of a novel inhibitor of phospholipase C-dependent processes on cell responsiveness. *J Pharmacol Exp Ther* **253**, 688–697.

Soboloff J, Spassova M, Xu W, He LP, Cuesta N & Gill DL (2005). Role of endogenous TRPC6 channels in Ca^{2+} signal generation in A7r5 smooth muscle cells. *J Biol Chem* **280**, 39786–39794.

Strubing C, Krapivinsky G, Krapivinsky L & Clapham DE (2001). TRPC1 and TRPC5 form a novel cation channel in mammalian brain. *Neuron* **29**, 645–655.

Tesfai Y, Brereton HM & Barritt GJ (2001). A diacylglycerol-activated Ca^{2+} channel in PC12 cells (an adrenal chromaffin cell line) correlates with expression of the TRP-6 (transient receptor potential) protein. *Biochem J* **358**, 717–726.

Thompson AK, Mostafapour SP, Denlinger LC, Bleasdale JE & Fisher SK (1991). The aminosteriod U-73122 inhibits muscarinic receptor sequestration and phosphoinositide hydrolysis in SK-N-SH neuroblastoma cells. *J Biol Chem* **266**, 23856–23862.

Tseng P-H, Lin H-P, Hu H, Wang C, Zhu MX & Chen C-S (2004). The canonical transient receptor potential 6 channel as a putative phosphatidylinositol 3,4,5-trisphosphate-sensitive calcium entry system. *Biochemistry* **43**, 11701–11708.

Welsh DG, Morielli AD, Nelson MT & Brayden JE (2002). Transient receptor potential channels regulate myogenic tone of resistance arteries. *Circ Res* **90**, 248–250.

Yu Y, Sweeney M, Zhang S, Platoshyn O, Landsberg J, Rothman A & Yuan JXJ (2003). PDGF stimulates pulmonary vascular smooth muscle cell proliferation by upregulating TRPC6 expression. *Am J Physiol Cell Physiol* **284**, C316–C330.

Zhang L & Saffen D (2001). Muscarinic acetylcholine receptor regulation of TRP6 Ca^{2+} channel isoforms. *J Biol Chem* **276**, 13331–13339.

Acknowledgements

This work was supported in part by National Institutes of Health (NIH) grant GM52019 and by Novartis Institutes for Biomedical Research, Horsham, UK.

Supplemental material

The online version of this paper can be accessed at:
DOI: 10.1113/jphysiol. 2005.103143
http://jp.physoc.org/cgi/content/full/jphysiol.2005.103143/DC1
and contains three figures:

Supplementary Figure 1. Effect of extracellular Ca^{2+} on whole-cell currents in TRPC6-expressing HEK 293 cells: NMDG buffer with 4 mM K^+

Supplementary Figure 2. Activation of TRPC6 in low- or high-Ba^{2+} buffer

Supplementary Figure 3. Model predictions for Ca^{2+} and monovalent current via TRPC6 channels

This material can also be found as part of the full-text HTML version available from http://www.blackwell-synergy.com